SLAC-PUB-754
June 1970
(EXP)

SLAC LARGE WIRE SPARK CHAMBER SPECTROMETER*

D. W. G. S. Leith and G. J. Luste

Stanford Linear Accelerator Center
Stanford University, Stanford, California 94305

I. INTRODUCTION

This is essentially a status report on the SLAC large aperture wire chamber spectrometer. The work has grown out of three years of experience with somewhat smaller systems and some of the results from those experiments are presented. The details of the large system are discussed and an analysis of its performance in a particular experiment, (viz., $\pi^- p \rightarrow \pi^+ \pi^- \pi^- p$ at 16 GeV/c) is presented. This spectrometer has been designed to study peripheral processes in the energy range (5-20) GeV/c, and as such would be of great utility in meson spectroscopy.

II. EXPERIENCE

The first wire chamber experiments at SLAC were started some 2-1/2 years ago by a SLAC-LRL collaboration[1] to study rho meson photoproduction. The spectrometer is shown in Fig. 1, (see Mark I) and consisted of four spark chambers with magnetostrictive readout, behind a 40" × 15" gap magnet. Rho production from hydrogen, deuterium and a succession of nuclear targets was measured at energies from 5 BeV to 16 BeV. The mass spectra, differential cross sections and decay distributions were studied, and the spin density matrix elements were determined from the decay data. Examples of the data are shown in Fig. 2. It is interesting to note that despite the

*Work supported by the U. S. Atomic Energy Commission.

(Presented at Experimental Meson Spectroscopy Conference, May 1-2, 1970, Philadelphia, Pa.)

severe limitations on the angular distributions at low energies, we were able to make significant contribution on the ρ^0 decay parameters, and provide strong support to the hypothesis that helicity is conserved in the ρ^0 decay.

Following these investigations, the SLAC Group B-C collaboration[2] set up the Mark II spectrometer, (see Fig. 1), to study the following processes:

$$\pi^- p \longrightarrow \pi^+\pi^- n$$
$$\pi^+\pi^- N^*$$
$$K^+K^- n$$
$$K^+K^- N^*$$
etc., at 8, 15 GeV/c.

The data was taken in January 1970. This time there were four wire chambers behind and three in front of the same 40" × 15" gap magnet, all chambers again with magnetostrictive readout. The wire chambers designed by F. Bulos and H. Lynch, were somewhat larger than the earlier versions, and operated superbly even at high repetition rates. The multiple spark efficiency held up above 95 percent at 8 sparks per event, operating at 180 pps. We also had a large aperture threshold Cerenkov counter[3] to select the kaon pairs from the pion pairs. Some very preliminary results from ~5% of the data using the on-line analysis program are shown in Fig. 3. The rho peak is clearly visible in the two pion mass spectrum, while the separation of the neutron and isobar in the missing mass plot is very good. This separation will be further improved in the off-line analysis, where the momentum resolution is improved by a factor of four. Typical values for the mass resolution at the rho is ~±6 MeV, and ~±60 MeV for the missing mass. Also shown are the ρ^0 decay distribution corrected for the angular acceptance, and the absolute differential cross section for elastic scattering. We took ≈2 hour check runs every other day to measure the elastic cross section as a calibration. The data from one of these runs is shown together with the classic measurements of Foley et al.[4] — the agreement is very good. The final decay distribution (i.e., a factor 20 more data) will allow the separation of the data into transverse or longitudinally polarized rho mesons, and also a study of the spin density matrix elements of the ρ^0 decay.

The work with these spectrometers has been fruitful, and plans to measure

$$\pi^- p \longrightarrow p\bar{p}n \text{ at } 15 \text{ GeV/c},$$

and

$$K^+ p \longrightarrow K\pi\pi N \text{ at } (10\text{-}13) \text{ GeV/c}$$

with a larger magnet are in progress, (see Mark III, Fig. 1). However, the mass acceptance and decay angular acceptance are severely limited by the size of the magnet aperture. Therefore, we have designed a large aperture wire chamber spectrometer with good mass resolution, good decay angular resolution and capable of gathering data at high rates. This system is described below.

III. THE LARGE APERTURE SPECTROMETER

We have proposed to build a large wire spark chamber spectrometer at SLAC[5] to study peripheral processes and in particular, meson spectroscopy. Monte Carlo investigations have been used to optimize the acceptance and evaluate the resolution of the system.[6-8] These studies are still in progress.

The present layout of the system is shown in Fig. 4. The basic elements of the system are (a) a large aperture analyzing magnet, (b) a superconducting solenoid with its field along the beam direction for supplementary momentum analysis, (c) spark chamber arrays, (d) trigger counters, (e) large aperture Cerenkov counter, (f) an on-line data acquisition system, and (g) an rf separated particle beam. Let us consider these one by one.

The magnet has a gap size of 110" × 70" with 1260 kg inches of field path. A sketch of the magnet is shown in Fig. 5 to give an idea of size. The drawing shows the pole piece of the magnet curved, with the production target at the center of the curvature. This innovation has been introduced to reduce fringe field corrections to the particle orbits. One of the most serious problems with these large spark chamber arrays is going to be the amount of computing required to reduce the raw data. Thus, the computing time per event has to be one of the main design criteria. Magnets of this aperture have normally very bad field distributions which would necessitate tracking (integration) through the magnet to establish the particle orbit (both for the track finding and momentum calculation) — a time consuming job (computer time, that is!). We have, therefore, attempted to design a large aperture magnet with as benign a fringe field as possible. The curved

pole tip means all tracks enter the field region normal to the magnet field lines and the exit fringe field effect is momentum dependent only (i.e., no production angle effects). On the same problem, we plan to use a superconducting mesh to "short out" the leaking flux lines, in addition to a conventional iron mirror plate. The eddy currents flowing in the mesh will be generated when the magnet is powered on, and the superconducting grid will then contain the leaking fringe field. Using these two methods it is hoped to have a magnetic field distribution which will not require time consuming integration to determine particle trajectories. A 1/10 scale model of the magnet has been constructed by H. Brechna and J. Alcorn at SLAC and studies are in progress to optimize the field configuration. Current results from this test magnet indicate that the nonuniformity in the integral field path may be expected to be as low as 2%.

The solenoid is a superconducting coil 60" in diameter and 100" long with its axis along the beam direction. Calculations have been performed for field strengths of 50 kg and 15 kg and the results are presented, however studies are still in progress trying to match the solenoid dimensions and field strength with the large magnet parameters. The solenoid picks up many of the large angle tracks that never enter the downstream magnet aperture, and even more important, it allows a measurement of the momentum of the slow forward particles which would be swept aside by the high field of the big analys s magnet. (It is this effect that causes the holes in our angular acceptance.)

All the large wire spark chambers have magnetostrictive readout, and vary in size from (100" × 60") for the front chambers, to (200" × 160") for the back chambers. These chambers will run at 180 pps to make use of SLAC's pulse rate characteristics, and have good multiple spark efficiency. The front chamber package is currently under construction,[9] and will be used as the back chambers early next year for an experiment with the Mark III setup (see Fig. 1). The experience gained with these already quite large chambers will dictate how to proceed with the big chambers. Each of the large chambers have a styrofoam plug in the region of the beam, since there will be (10-20) particles through the chambers during the 1.5 μsec beam pulse. Proportional spark chambers, with a time resolution of ~ 80 nsec, will be used to readout the spark coordinates in this "dead" region for each trigger. The chambers in the solenoid are a mixture of proportional chambers and conventional wire chambers.

The trigger logic is formed around two large picket fence hodoscopes, one immediately behind the analyzing magnet and the other behind the last wire plane. In addition to being the basic element in the trigger signal, these counters help in forming "roads" for track finding in the spark chamber data.

The large aperture Cerenkov counter is a "monster" version of our present counter[3] which has been shown to work very well. The on-line data acquisition system has to be capable of handling high data rates (i.e., ~ 100 Kbytes/sec) and have enough calculational power to perform full reconstruction on a sample of the events. However, we will not describe this system in any detail here. The high energy beam will be able to deliver separated $K^{\pm}$, $\bar{p}$ with momenta to 15 GeV/c, and with flux's in excess of 10^3/sec.

In order to evaluate the performance of this spectrometer we have studied the acceptance and resolution with a Monte Carlo simulation of the reaction:

$$\pi^- p \longrightarrow A^- p \text{ at 16 GeV/c}$$

where

$$A^- \longrightarrow \rho^0 \pi^-, \ \rho^0 \longrightarrow \pi^+ \pi^-.$$

The A and ρ^0 were represented by Breit Wigner amplitudes, and the proton differential cross section was generated as e^{-8t}. The Monte Carlo events were able to reproduce the distributions of real bubble chamber data — the SLAC 16 GeV/c $\pi^- p \longrightarrow \pi^+ \pi^- \pi^- p$ data.[10]

We choose this reaction in that it is a typical high energy diffractive process, to be compared with $K\pi\pi(1300)$ production in KN reactions, or $N\pi\pi(1400)$ in NN interactions. Furthermore, the three particle decays allows a real test of the angular acceptance of the system. It turns out that a major difficulty in such a spectrometer system is how to measure the decays which involve both fast and slow particles. This dichotomy can lead to low overall acceptance and serious dead regions in decay distributions. This is specially true for the three particle decay events being considered here. We believe that one very interesting solution to this problem is the use of a solenoid magnet with longitudinal magnetic field with an internal spark chambers system.

The acceptance of the spectrometer has been evaluated for two solenoid fields - 15 kg and 50 kg, respectively. The criteria applied to each event

is that the three pion tracks must either go through the big downstream magnet and be recorded in the back spark chamber or be measured in the solenoid by sufficient chambers to allow reconstruction of a track and calculate the momenta to better than 5% for the 15 kg tests, or 1-1/2% for the 50 kg tests. Since particles with momentum greater than 2 GeV/c will be measured by the forward system, the 5% cut-off is a tolerable limit from a physics point of view.

However, a superconducting solenoid with B = 50 kg and a diameter of 1.5 meters has the advantage that it can trap the helix trajectory of all particles with a transverse momentum of 550 MeV/c or less. This corresponds to about 80% of all strong interaction secondaries, since $P_\perp$ has a relatively invariant spectrum. In addition, this solenoid system has the capability of detecting the peripheral proton in the final state, so allowing for the study of charged meson decay with one neutral decay particle.

The overall acceptance for the 50 kg case is ~95%, while it is ~75% for 15 kg and drops to ~40% without the solenoid. In this case many of the slow pions, (i.e., $\lesssim$ 2 GeV/c), do not get through the system, resulting not only in a reduced overall efficiency, but causing holes in specific angular regions.

In Fig. 6 we show the 3π and 2π mass spectra and the associated detection efficiency as a function of mass. The upper curve refers to the 50 kg solenoid field case, while the lower curve refers to no solenoid field. A quite dramatic increase in detection efficiency is shown, and holds up with reasonable efficiency up to masses of ~3500 MeV. We should note that the momentum transfer distribution also shows a good detection efficiency.

Figure 7 illustrates the corresponding efficiency curves for the helicity frame decay $\cos\theta$. Here the loss of the slow pions for the no-solenoid system has the dramatic effect of depleting the $|\cos\theta| \sim 1.0$ regions in the ρ decay, and $\cos\theta \sim +1.0$ region in the A decay. This makes a spin parity analysis in many cases very difficult. The upper curves show that these forward - backward holes are filled in when the solenoid is included. The dashed curve shows the efficiency when the solenoid field is 15 kg, while the solid line refers to the 50 kg field acceptance.

The mass resolution and missing mass resolution are $\sim \pm 6$ MeV and $\pm$ 50 MeV respectively, including multiple scattering, assuming that we can measure the secondary particles to $\pm$ 1/2% in momentum and $\pm$ 1 mrad in angles, while the beam is known to $\pm$1/4% in momentum and to the same angular accuracy.

IV. CONCLUSION

In conclusion, a large aperture spectrometer with exciting possibilities for meson spectroscopy has been presented and its performance in a given experimental situation analyzed in detail. The parameters of this system are still being optimized in a constant attempt to reduce the cost.

REFERENCES

1. F. Bulos, W. Busza, R. Giese, R. R. Larsen, D.W.G.S Leith, B. Richter, V. Perez-Mendez, A. Stetz, S. H. Williams, and M. Beniston, Phys. Rev. Letters 22, 490 (1969); D.W.G.S. Leith, Invited talk presented at 3rd Interantional Conf. on High Energy Physics and Nuclear Structure, Columbia University, New York, September 1969. Also Report No. SLAC-PUB-679, Stanford Linear Accelerator Center, Stanford University, Stanford, California.
2. F. Bulos, R. Carnegie, G. Fischer, E. Kluge, D.W.G.S. Leith, H. Lynch, B. Ratcliff, B. Richter, H. H. Williams, and S. Williams.
3. A. Kilert, D.W.G.S. Leith, H. H. Williams (to be published).
4. K. J. Foley et al., Phys. Rev. Letters 11, 425 (1963).
5. D. W.G.S. Leith, Large Wire Spark Chamber Proposal.
6. G. J. Luste and L. Madansky, Group B Physics Note 34, $\pi p \longrightarrow \pi \ldots \pi p$ and "A_1-type" Resonance Kinematics fron 6 to 22 GeV/c.
7. G. J. Luste and L. Madansky, Group B Physics Note 36, A_1 - A_2 Enhancement Efficiencies for the Proposed Large Magnet - Spark Chamber Facility at SLAC.
8. G. J. Luste, Group B Physics Note 43, Solenoid-Spark Chamber System.
9. Work is being done on this chamber package by R. Carnegie, A. Kilert, D.W.G.S. Leith, and S. H. Williams, SLAC Group B.
10. J. Ballam, A. D. Brody, G. B. Chadwick, Z.G.T. Guiragossian, W. B. Johnson, R. R. Larsen, D.W.G.S. Leith, and K. Moriyasu, Report Nos. SLAC-PUB-475 and 627, Stanford Linear Accelerator Center, Stanford University, Stanford, California.

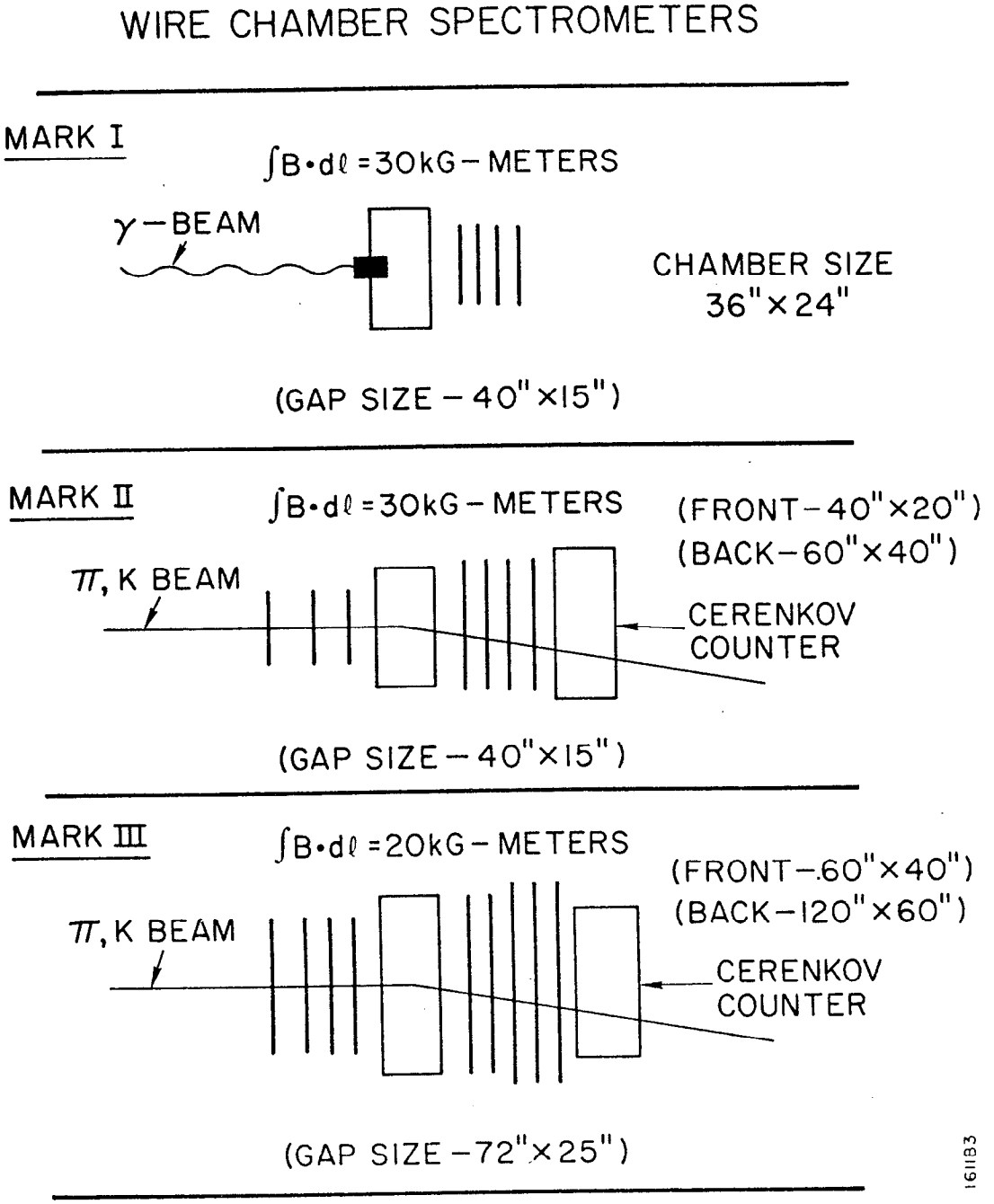

Figure 1 A schematic of the wire chamber spectrometers which have been, or are currently being, built by SLAC Groups B-C. (a) Mark I system was used to study photo-rho production from (5-16) GeV. (b) Mark II has been used to study rho production by pions at 8, 15 GeV/c. Production of $K\bar{K}$ and $p\bar{p}$ pairs is also being studied with the aid of the large aperture Cerenkov counter. (c) Mark III is being assembled for a study of the Q region in K^+p interactions, in the momentum region from 10-14 BeV/c.

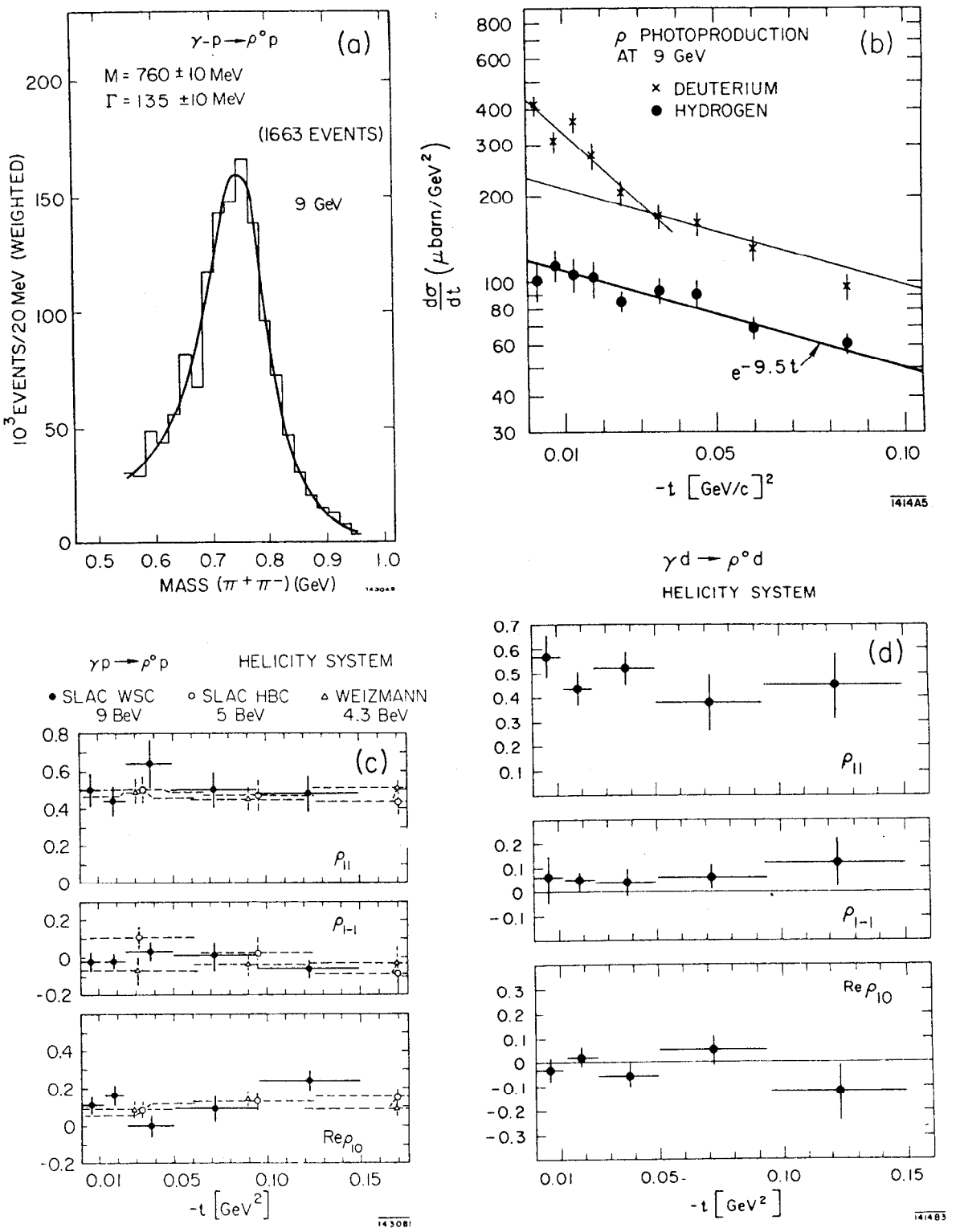

Figure 2 Some results from experiments with the Mark I system. In (a) the dipion mass distribution for the reaction $\gamma p \longrightarrow \pi^+\pi^- p$, at 9 BeV, is shown. (b) The differential cross section for rho photoproduction from hydrogen and deuterium at 9 BeV. (c) and (d) show the spin density matrix elements for rho decays in photoproduction on hydrogen and deuterium, respectively. (The ρ_{ij} are evaluated in the helicity system.) Data from two HBC experiments, at a somewhat lower energy, is shown for comparison.

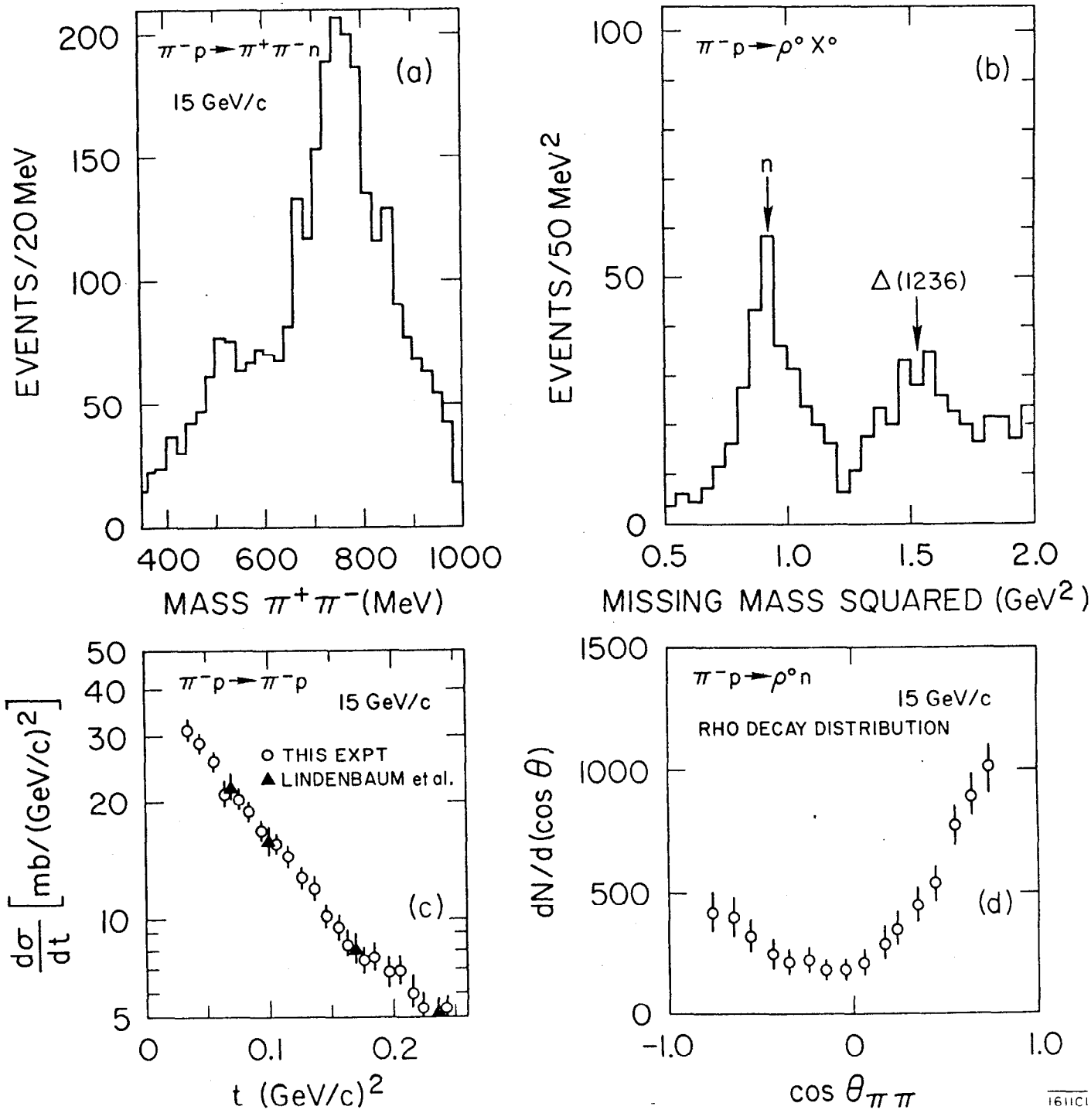

Figure 3 Some preliminary data of ~5% of the experiment, from on-line analysis: (a) The dipion mass spectrum for $\pi^- p \to \pi^+ \pi^- n$ at 15 GeV/c; (b) the missing mass squared distribution for $\pi^- p \to \rho^0 X^0$, showing clean separation between the neutron events and the N* (1236) isobar production; (c) an absolute measurement of the elastic scattering differential cross section at 15 GeV/c, taken every other day as a calibration. Data from Foley et al., is shown for comparison; (d) the rho decay angular distribution for the reaction $\pi^- p \to \rho^0 n$ at GeV/c, in the rho rest frame, corrected for the angular acceptance of the spectrometer. Note the cut-off for $|\cos \theta_{\pi\pi}| > .8$, where the acceptance has essentially gone to zero.

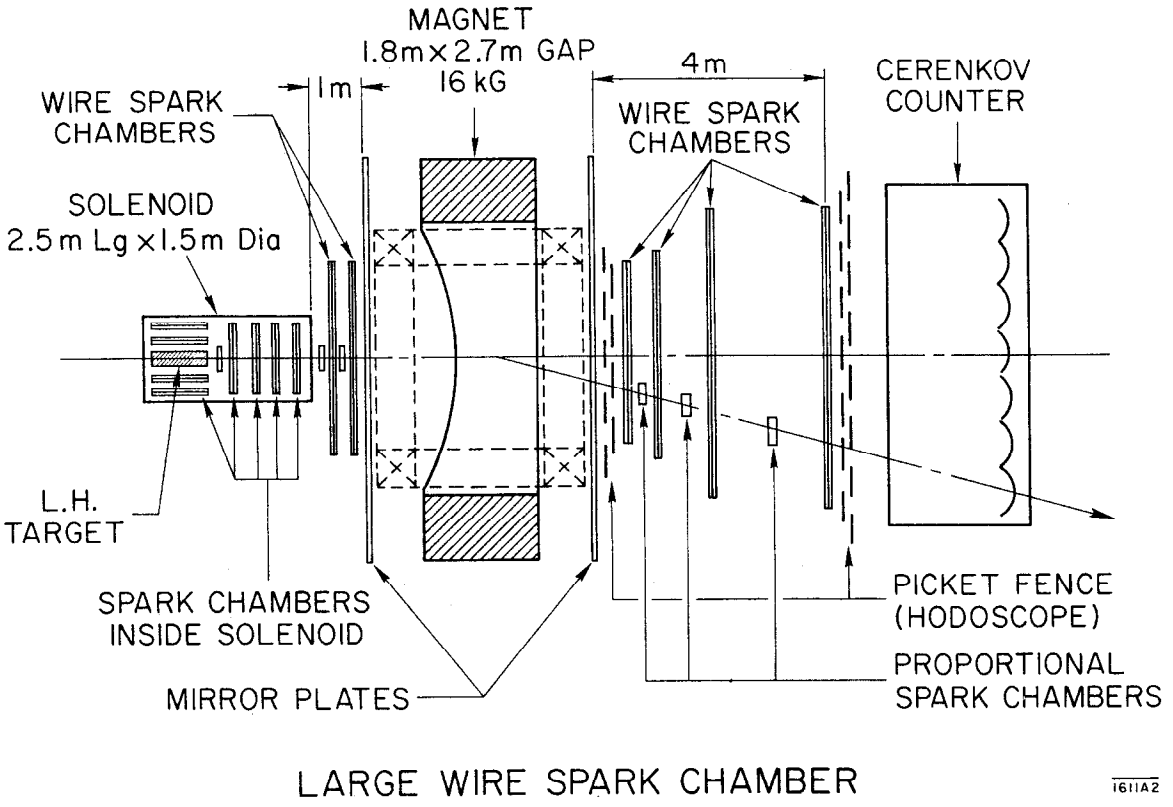

Figure 4 Schematic layout of the proposed large aperture spectrometer. The analysis system consists of two separate field volumes, the large aperture magnet downstream and a superconducting solenoid around the target. The solenoid is 60" in diameter, and 100" long with the magnetic field of ~50 kg, along the beam line. A system of cylindrical, and plane, spark chambers measure the slow particles within the solenoid, while a series of conventional wire chambers in front and behind the large magnet (110"×70" gap) measure the forward going particles. The chambers range in size from (100"×60") in front, to (200"×160") behind. Since the large chambers have styrofoam plugs in the region of the beam, there are several proportional chambers throughout the system to provide spark information on each event within this "dead" region. Two large "picket-fence" hodoscopes provide the information for the trigger logic and finally, a large aperture threshold Cerenkov hodoscope counter allows separation of π's, K's, and $\bar{p}$'s depending upon the operating range.

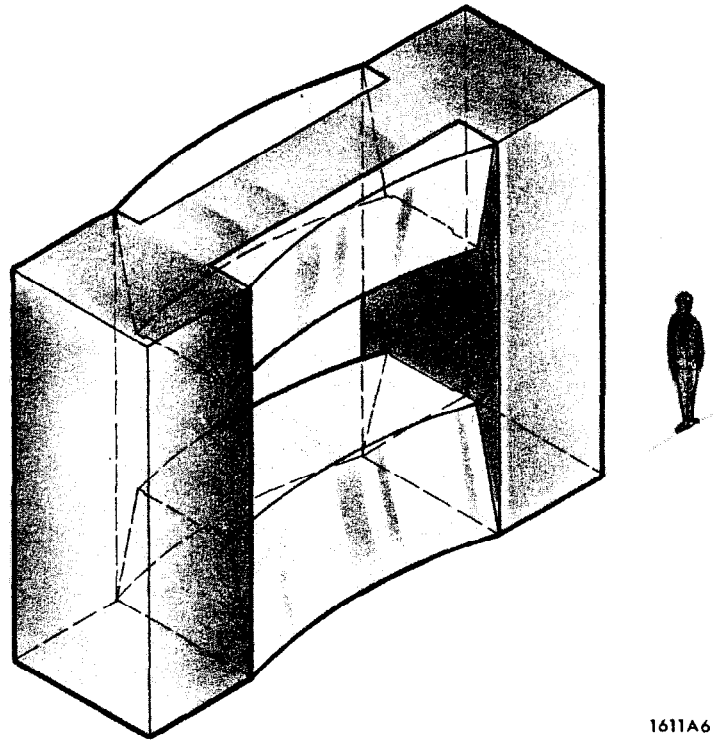

Figure 5 Schematic of the large downstream magnet. (For details see text.)

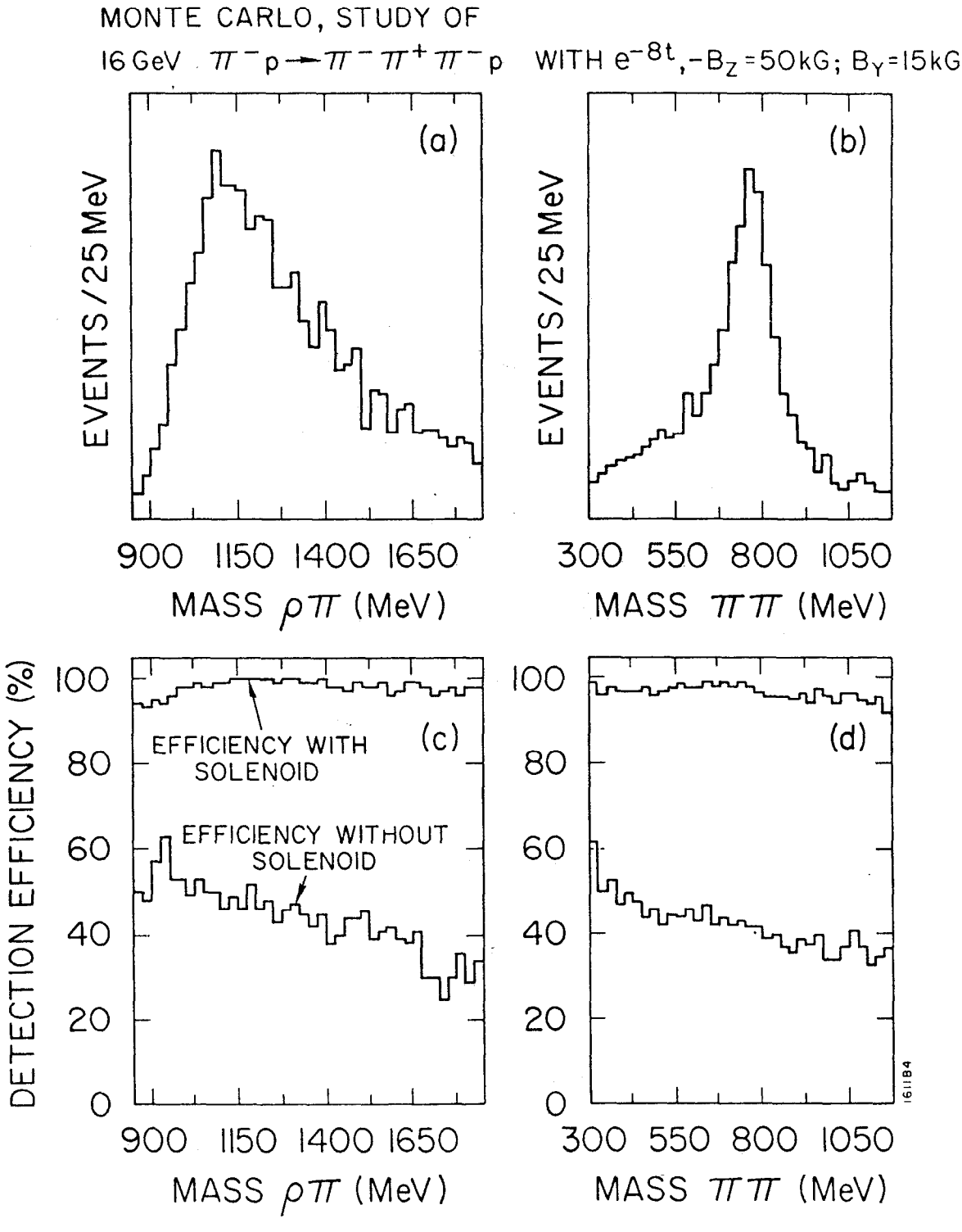

Figure 6 The mass spectra detected by this system, as predicted by a Monte Carlo simulation of the reaction $\pi^- p \rightarrow \pi^+ \pi^- \pi^- p$ at 16 GeV/c. (a) and (b) are the 3π and 2π mass spectra respectively, while (c) and (d) show the detection efficiency of the system as a function of mass. The lower curve shows the acceptance of the system without the solenoid, while the upper curve refers to the system including the solenoid, with 50 kg longitudinal field.

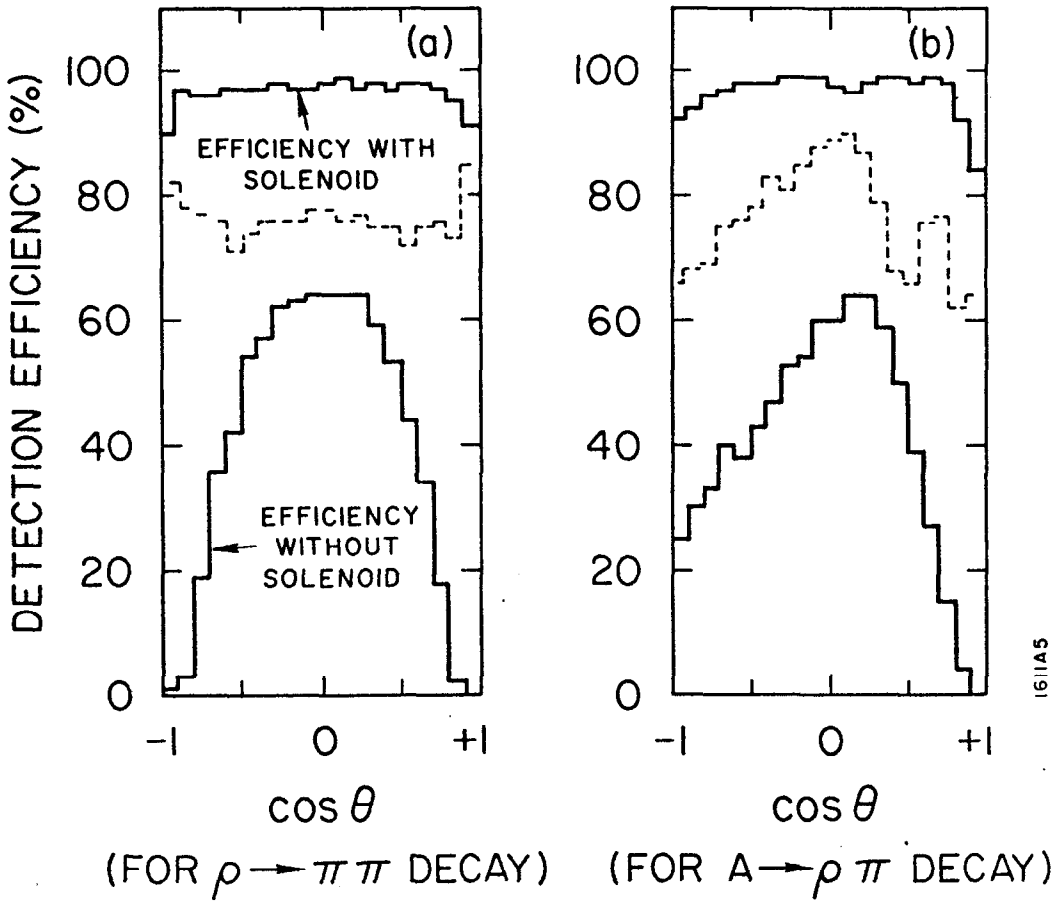

Figure 7 The angular detection efficiency is shown for (a) the two-pion distribution in the rho rest frame, and (b) the three pion decay distribution in the $\rho\pi$ rest frame. The upper (lower) solid curve refers to the system including (excluding) the 50 kg solenoid field. Notice that the problematic "holes" in the decay angular acceptance have disappeared. The dashed curves show the efficiency, for the solenoid field reduced to 15 kg.